Ionic Currents in Dispersed Chemoreceptor Cells of the Mammalian Carotid Body

J. UREÑA, J. LÓPEZ-LÓPEZ, C. GONZÁLEZ, and J. LÓPEZ-BARNEO

From the Departamento de Fisiología y Biofísica, Facultad de Medicina, Universidad de Sevilla, 41009 Sevilla, Spain

ABSTRACT   Ionic currents of enzymatically dispersed type I and type II cells of the carotid body have been studied using the whole cell variant of the patch-clamp technique. Type II cells only have a tiny, slowly activating outward potassium current. By contrast, in every type I chemoreceptor cell studied we found (a) sodium, (b) calcium, and (c) potassium currents. (a) The sodium current has a fast activation time course and an activation threshold at ~ -40 mV. At all voltages inactivation follows a single exponential time course. The time constant of inactivation is 0.67 ms at 0 mV. Half steady state inactivation occurs at a membrane potential of ~ -50 mV. (b) The calcium current is almost totally abolished when most of the external calcium is replaced by magnesium. The activation threshold of this current is at ~ -40 mV and at 0 mV it reaches a peak amplitude in 6–8 ms. The calcium current inactivates very slowly and only decreases to 27% of the maximal value at the end of 300-ms pulses to 40 mV. The calcium current was about two times larger when barium ions were used as charge carriers instead of calcium ions. Barium ions also shifted 15–20 mV toward negative voltages the conductance vs. voltage curve. Deactivation kinetics of the calcium current follows a biphasic time course well fitted by the sum of two exponentials. At -80 mV the slow component has a time constant of 1.3 ± 0.4 ms whereas the fast component, with an amplitude about 20 times larger than the slow component, has a time constant of 0.16 ± 0.03 ms. These results suggest that type I cells have predominantly fast deactivating calcium channels. The slow component of the tails may represent the activity of a small population of slowly deactivating calcium channels, although other possibilities are considered. (c) Potassium current seems to be mainly due to the activity of voltage-dependent potassium channels, but a small percentage of calcium-activated channels may also exist. This current activates slowly, reaches a peak amplitude in 5–10 ms, and thereafter slowly inactivates. Inactivation is almost complete in 250–300 ms. The potassium current is reversibly blocked by tetraethylammonium. Under current-clamp conditions type I cells can spontaneously fire large action potentials. These results indicate that type I cells are excitable and

Address reprint requests to Dr. J. López-Barneo, Departamento de Fisiología y Biofísica, Facultad de Medicina, Avenida de Sánchez Pizjuán, 4, 41009 Sevilla, Spain. Dr. J López-López and Dr. C. González' permanent address is Departamento de Bioquímica y Biología Molecular y Fisiología, Facultad de Medicina, Universidad de Valladolid, C/ Ramón y Cajal 5, 47005 Valladolid, Spain.

have a variety of ionic conductances. We suggest a possible participation of these conductances in chemoreception.

INTRODUCTION

The mammalian carotid bodies are paired organs that sense the level of oxygen tension (pO_2) in arterial blood. This sensory information is sent to the central nervous system where it induces an adequate ventilatory response (De Castro, 1928; Heymans et al., 1930; Fitzgerald and Lahiri, 1986). Among the different structures of the receptor complex (glomus or type I cells, subtentacular or type II cells, and nerve endings) type I cells, the most numerous in the carotid body, are presumably the primary chemoreceptors. Type I cells are rich in secretory granules containing dopamine, norepinephrine, and other neurotransmitters and they establish chemical synapses with nerve endings. A decrease in pO_2 ultimately results in transmitter release by type I cells and excitation of the afferent fibers of the carotid sinus nerve (see for reviews Eyzaguirre and Zapata, 1968; Fidone and González, 1986).

The mechanism involved in the transduction of the hypoxic stimulus is unknown. It has been recently shown that either low pO_2 or high external potassium can induce the release of dopamine from type I cells, which is dependent on external calcium and is inhibited by calcium channel blockers (Fidone et al., 1982; Obeso et al., 1987). These data suggest that, in concordance with the mechanism of stimulus-secretion coupling in many secretory systems, membrane depolarization may play a part in the response of type I cells to hypoxia.

The present research work was undertaken to characterize the electrical properties of the cellular elements of the carotid body and to test the hypothesis that membrane ionic conductances could be altered by changes in pO_2. From an electrophysiological viewpoint type I cells are practically unknown. Some previous electrophysiological studies have been performed using intracellular recording microelectrodes, but they are somewhat confusing and inconclusive because they were probably done on cells damaged by the microelectrode impalement. It has been reported that type I cells are nonexcitable and their electrical parameters are unaltered by hypoxia (Eyzaguirre et al., 1983; Acker and Pietruschka, 1977). These experiments were, however, done on cells with an average resting potential (-20 mV) that is low enough to produce complete inactivation of the voltage-dependent membrane ionic conductances.

We have performed experiments in acutely dispersed cells of the carotid body subjected to whole-cell patch clamp, which is a technique that permits accurate electrical measurements in small cells (Hamill et al., 1981). Our data demonstrate that type I cells have a variety of voltage-dependent ionic channels and that they are able to generate large sodium- and calcium-dependent action potentials. Type II cells are unexcitable and on depolarization only generate a small outward current. This article concentrates on the full description of the sodium, calcium, and potassium currents of type I cells. The following article illustrates that in these cells potassium channel activity is reversibly decreased by hypoxia, which may be the membrane mechanism responsible for chemotransduction. Some of this work has already appeared in a short report (López-Barneo et al., 1988).

METHODS

Cell Dissociation and Culture

Experiments were performed on cells dissociated from rabbit carotid bodies. The protocol used for cell dissociation was worked out at the University of Valladolid in collaboration with Dr. Benito Herreros.

Animals were anesthetized and the whole region of the carotid artery bifurcation was removed. Four carotid bodies were dissected under a microscope, cleaned, and then each one of them was cut into two or three small pieces. The tissue was placed in a vial with 2 ml of a Ca^{2+}- and Mg^{2+}-free Tyrode solution of the following composition, in millimolar: 140 NaCl, 4.7 KCl, 5 Na pyruvate, 3 sucrose, 5 glucose, and 10 HEPES. This solution also contained trypsin (2 mg/ml), collagenase (2 mg/ml), and DNase (0.5 mg/ml). Every 10 min the tissue was triturated. After 20 min at 37°C the vial was centrifuged at 800 g for 5 min. The pellet was resuspended in another 2 ml of the same solution with collagenase (4 mg/ml), DNase (0.5 mg/ml), and albumin (5 mg/ml), and kept at 37°C for 20 min. The tissue was triturated every 10 min. At the end of the incubation period the preparation was washed twice with the Ca^{2+} and Mg^{2+}-free solution to remove the enzymes, and the final pellet was resuspended in 5 ml of minimum essential medium supplemented with glutamine (1%), penicillin-streptomicin (2%), and fetal calf serum (5%). Cells were plated on slivers of glass cover slips treated with poly-*l*-lysine and kept in a CO_2 incubator at 37°C until use (4–48 h after plating). After the cells were dissociated, most of them had a round shape and two distinct populations could be easily distinguished. Type I cells had a diameter between 9 and 13 μm and a typical birefringence appearance under the light microscope. A second population of cells, classified as putative type II cells, had a smaller and more uniform diameter (between 5 and 7 μm). These two cell types also had clear differences in their electrical properties (see Results). After 48 h in culture many cells began to show growing processes and acquired a bipolar or an irregular shape.

Solutions

During the experiments a cover slip was transferred to a small chamber that had a continuous flow of solution that could be changed in ~15–20 s. The composition of the recording solutions is shown in Table I. In the text and figure legends solutions are indicated as external/internal. TTX (500–1,000 nM) was added to the external solution to block Na channels and in most experiments 3 mM Mg-ATP were added to the internal solution to retard wash-out of Ca channels (Kostyuk, 1984; Forscher and Oxford, 1985; Cota 1986). In some experiments designed to record K currents, the internal solution contained a known concentration of free Ca^{2+}, which was obtained using Ca-EGTA buffers. The concentrations of Ca and EGTA used in these experiments are indicated in the figure legends. Unless otherwise noted, the pH of the external and internal solutions were adjusted to 7.4 and 7.2–7.3, respectively. Experiments were performed at room temperature (20–25°C).

Recording Techniques

Ionic currents of type I cells were recorded using the whole-cell variant of the patch-clamp technique (Hamill et al., 1981). Patch electrodes were usually fabricated from soft hematocrit capillaries (Hirschmann, Federal Republic of Germany) but in several experiments borosilicate glass (Kimax 51) was also used. In our experimental conditions, current recorded with both types of electrodes were indistinguishable. The electrode tip was fire polished on a microforge and electrode resistance varied between 1 and 2 MΩ. The patch-clamp amplifier used in most experiments was built by us following the standard design (Sigworth, 1983; Mat-

teson and Armstrong, 1984; Armstrong and López-Barneo, 1987). The current-to-voltage converter was a Burr-Brown OPA 111 (Tucson, AZ). Frequency response was improved by using low resistance electrodes, electronic compensation of series resistance, and a relatively low feedback resistance (100 MΩ). Current-clamp recordings were done in some cells using a List patch-clamp amplifier (model LPC-7; Adams and List Associates, Ltd., Great Neck, NY).

Data Acquisition and Analysis

An IBM-PC/AT computer interfaced to the analog electronics was used for pulse generation and for acquisition, display, storage, and analysis of the data. The interface, fabricated in our laboratory, is built on two IBM prototype cards directly connected to the expansion bus of the computer (Ureña et al., 1989). The pulse generator has an 8 bit digital-to-analog converter (DCA 0808; Analog Devices, Inc., Norwood, MA) and a programmable peripheral interface (PPI 8255A-5; NEC Microcomputers, Inc.) with the ports programmed in output

TABLE I

Composition of Solutions

	NaCl	KCl	CaCl$_2$	MgCl$_2$	External BaCl$_2$	CdCl$_2$	TEACl	HEPES
140 Na	140	2.7	2.5–10	—	—	—	—	10
140 Na, 10 Ba	140	2.7	—	—	10	—	—	10
140 Na, 9 Mg	140	2.7	1	9	—	—	—	10
140 Na, 0.5 Cd	140	2.7	1.5	—	—	0.5	—	10
100 Na, TEA	100	2.7	5	—	—	—	40	10

	NaCl	KCl	K-glutamate	KF	Internal CsCl	CsFl	MgCl$_2$	HEPES	EGTA
130 K	—	30	80	20	—	—	2	10	5–10
130 Cs	—	—	—	—	110	20	2	10	5–10
90 Cs, 40 Na	40	—	—	—	70	20	2	10	5–10

All values are given in millimolar.

mode (Peatman, 1977; Liu and Gibson, 1986). Current signals are digitized in a 12 bit analog-to-digital converter (ADC, AD578; Analog Devices, Inc.). The 12 lines of parallel output of the ADC are transferred to the computer RAM memory by means of a PPI chip with the ports programmed in input mode (Peatman, 1977). The acquisition sampling interval can be changed by the program to values between 20 and 500 μs. Digitized current signals are displayed in an oscilloscope after being converted into analog form. In this system each current trace is defined by 500 samples. In most experiments linear ionic and capacity currents were subtracted using a P/4 procedure (Bezanilla and Armstrong, 1977). During analysis tail currents were fitted with one or the sum of two exponentials using a least-squares procedure.

RESULTS

The data presented in this paper were obtained from over 150 type I chemoreceptor cells subjected to voltage clamp. These cells had an average capacitance of 7.27 ± 2.26 pF (mean ± SD, n = 50). The electrical properties of type II cells, which generate only a tiny outward current, are presented at the end of the paper.

Ionic Current Components

The major components of ionic current recorded in type I cells are shown in Fig. 1. With the standard high K internal solution, depolarization to 30 mV from a holding potential of -70 mV elicited a fast inward current followed by a slower outward current (Fig. 1 A). At the repolarization of the 8-ms pulse the current changes suddenly in direction and a large inward tail current was recorded. This response pattern was observed in every cell studied although the amplitude of the different current components varied from cell to cell.

The outward current was mainly carried by K ions since it disappeared when all the K in the pipette solution was replaced by Cs. In this condition (Fig. 1 B) a fast and sustained inward current, followed by an inward tail, were recorded by a depo-

A   140 Na, 2.5 Ca // 130 K

B   140 Na, 10 Ca // 130 Cs

C   140 Na, 10 Ca, TTX // 130 Cs

2 ms
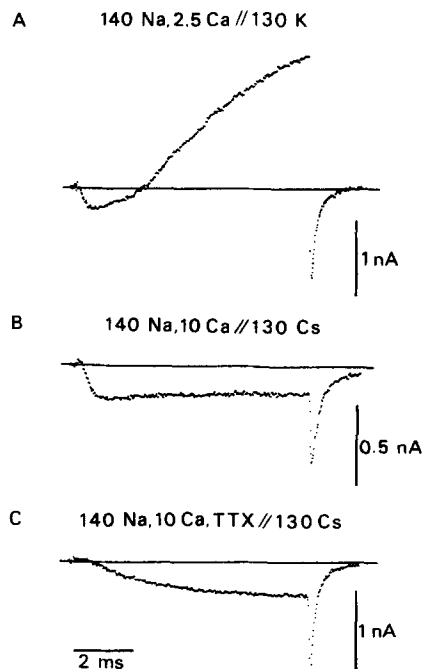
FIGURE 1. Major current components in type I cells. (A) Current recorded during a voltage step to 30 mV with return to the holding potential (HP) of -70 mV after 8 ms. (B) Blockade of the outward potassium current by internal cesium. Pulse to 20 mV and HP of -80 mV. Calcium current is recorded in isolation by application of the same voltage step in the presence of TTX (C). Solution composition was as indicated next to each trace. Experiments EN1988J (A) and EN2188J (B and C).

larization to 20 mV from a holding potential of -80 mV. The addition of TTX to the external solution (Fig. 1 C) abolished the fast component of the inward current, which indicates that it was due to the activity of Na channels. However, the slowly activating inward current and the tail remained unaltered. These two last current components were the result of the activity of Ca channels since, as will be shown below, they disappeared after replacement of external Ca by Mg, or when 0.5 mM Cd was added to the external solution. These results indicate the existence in type I chemoreceptor cells of voltage-dependent Na, Ca, and K channels.

Properties of the Sodium Current

Current-voltage relations. Na currents were recorded in isolation in cells where internal K ions were replaced by Cs (or a mixture of Cs and Na), and Ca channels

were blocked by external Mg or Cd. A family of Na current records obtained by depolarizations to the indicated membrane potentials is shown in Fig. 2 A. The holding potential was -80 mV and the internal solution contained 40 mM Na. Na current had a voltage-dependent fast activation time course, at 0 mV it reached a peak in ~0.6–0.7 ms, and then it inactivated completely. Current was inward at membrane potentials more negative than E_{Na} and outward with more positive membrane potentials.

The current-voltage relation for this experiment is shown in Fig. 2 B, where the peak current amplitude is plotted as a function of the pulse membrane potential (V_M). Activation threshold was ~-40 mV, the peak of the I-V curve occurred at a V_M
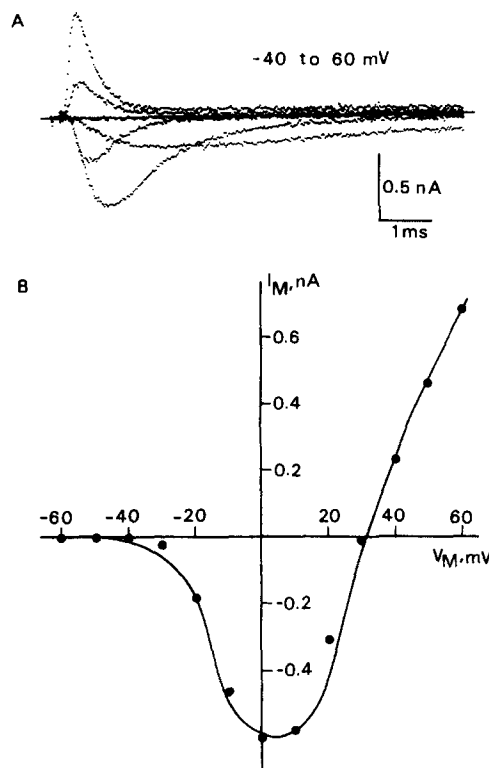
FIGURE 2. Family of sodium currents recorded during depolarizations to -40, -20, 0, 20, 40, and 60 mV from a HP of -80 mV (A). Peak current amplitude as a function of the membrane potential is plotted in B. The continuous line was fitted by eye. Solutions (in millimolar): 140 Na, 0.5 Cd//90 Cs, and 40 Na. Experiment MZ0288M.

of 0 to $+10$ mV, and the reversal potential was at $+32$ mV, which was only 1 mV apart from the E_{Na} value predicted by the Nernst equation. Although inward Na currents were observed in every cell studied the amplitude varied from cell to cell. The maximal Na current amplitude recorded in cells without internal Na was 0.46 ± 0.2 nA (mean ± SD, $n = 6$).

Inactivation. In type I cells inactivation of the Na current was, as in other preparations, a voltage-dependent process. Fig. 3 A illustrates the voltage-dependence of steady-state inactivation by measuring the peak Na current elicited by a depolarization to 10 mV as a function of V_M during a 50-ms conditioning prepulse. In the ordinate, current amplitude is normalized with respect to its value in the absence of

prepulse. Half steady-state inactivation was at ~ -50 mV, and at -25 mV the non-inactivated fraction of I_{Na} was <10%. The inset in Fig. 2 B illustrates that at 0 mV inactivation was complete in <6 ms and that its time course could be well fitted by a single exponential with a time constant of 0.67 ms. The plot in the same figure shows that the time constant of inactivation decreased with membrane depolarization.

Closing kinetics. The closing of Na channels was studied in a few cells by the application of short depolarizing pulses (0.5–1 ms), which prevented the development of inactivation, and the recording of tail currents at the instant of repolarization. Na tails were well fitted by single exponentials and at -80 mV the time con-
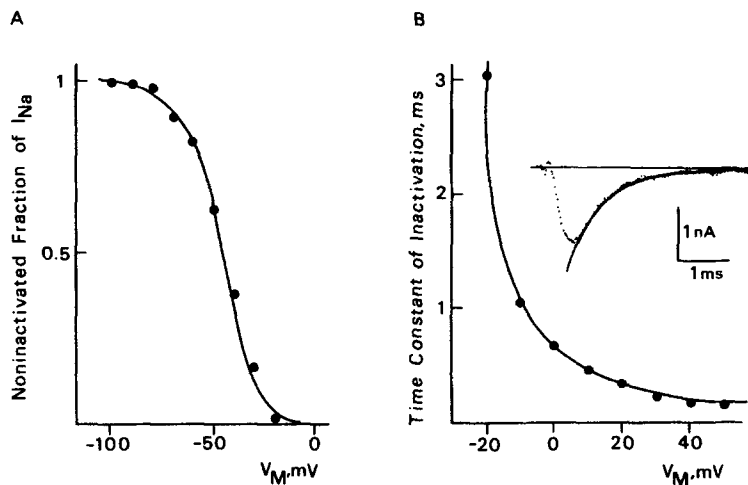
FIGURE 3. (A) Steady-state inactivation of sodium currents. The plot represents normalized peak current amplitude obtained during a test step depolarization to 10 mV as a function of the membrane potential during a 50-ms conditioning prepulse. (B) Time course of inactivation. The inset is a sodium current recorded by a voltage step to 0 mV. Inactivation is well fitted by an exponential with a time constant of 0.67 ms. The plot represents the time constant of inactivation (ordinate) measured in currents recorded at various membrane potentials (abscissa). Lines were fitted by eye. HP, -80 mV. Solutions (in millimolar): 140 Na and 0.5 Cd//130 Cs. Experiments EN2888J (A) and FE0388J (B).

stant was between 60 and 70 μs. Thus, these results indicate that type I chemoreceptor cells have a prominent Na current with properties similar to those found in other electrically excitable cells.

Properties of the Calcium Current

Identification of the current. Ca currents were recorded in cells dialyzed with the 130 Cs solution. Fig. 4 A shows a trace of inward current in this experimental condition and with 10 mM Ca in the external solution. The pulse current was followed by a large inward tail current. Exposure to a different external solution with less Ca (9 mM Mg, 1 mM Ca) produced a marked reduction of the steady-state pulse current and the tail, although a small component of inactivating inward Na current

A

140 Na//130 Cs

B

140 Na,TTX//130 Cs

9 Mg,1 Ca

10 Ca

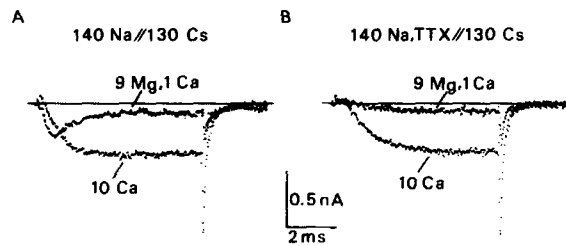9 Mg,1 Ca

10 Ca

0.5 nA

2 ms

FIGURE 4. Identification of the calcium current. (A) Inward current recorded with the 140 mM Na, 10 mM Ca external solution during a voltage step to 0 mV. On replacing calcium with magnesium (9 mM Mg, 1 mM Ca) the steady inward current and the tail almost disappear but a small component of transient sodium current remains. In the presence of TTX (B) the isolated calcium current recorded in 10 mM Ca is almost abolished after the introduction of the 9 mM Mg, 1 mM Ca solution in the bath. HP, −80 mV. Solutions were as indicated in the figure. Experiments EN2788J (A) and EN2588J (B).

remained. After Na channels were blocked with TTX in another cell (Fig. 4 B), Ca currents could be recorded in total isolation. This current activates slowly and at 0 mV it reaches a maximum in ~8 ms. Fig. 4 B also illustrates the almost complete disappearance of the pulse current and the tail after replacement of external Ca by Mg. In other experiments with low external Ca (1.5 mM) the addition of 0.5 mM Cd to the external solution completely abolished the Ca current (see Fig. 2).

Current-voltage relations. Fig. 5 (left column, 10 Ca) shows calcium currents recorded at various membrane potentials. Current generated during the pulse, indicated between the arrows, activates more rapidly at more depolarized levels and is followed by a fast tail whose amplitude increases with the amplitude of the depolarization. These tails are due to the flow of Ca ions through the channels that were open during each pulse, and their time course reflects that of the closing of the Ca channels. Current amplitude measured at the end of the pulse as a function of pulse

V_M,mV

10 Ca
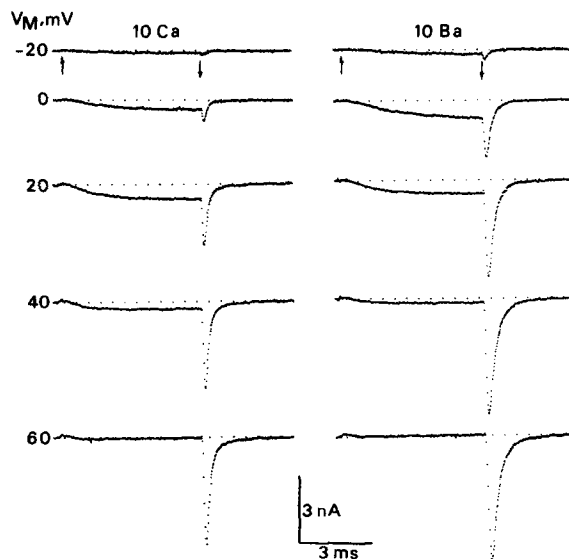
10 Ba

−20

0

20

40

60

3 nA

3 ms

FIGURE 5. Current through calcium channels carried by calcium and barium ions. Currents are the result of depolarizations to the membrane potentials indicated next to each trace with 10 mM Ca or 10 mM Ba in the external solution. The arrows indicate the onset and the end of the voltage steps. All traces are from the same cell. HP, −80 mV. Solutions (in millimolar): 140 Na, 10 Ca (10 Ba), and TTX//130 Cs. Experiment MZ0288K.
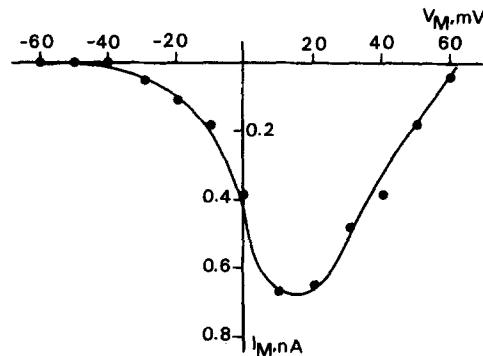
FIGURE 6. Calcium current-voltage relation. The current measured at the end of 8-ms pulses is plotted as a function of the pulse membrane potential. The line was fitted by eye. HP, −80 mV. Solutions (in millimolar): 140 Na, 10 Ca, and TTX//130 Cs. Experiment MZ0288K.

membrane potential is plotted in Fig. 6. This *I-V* plot shows that the activation threshold was at ~ -40 mV and that the maximal inward current was obtained at $+10$ to $+20$ mV. At these V_M values the average amplitude of the Ca current measured with 10 mM external Ca was 0.4 ± 0.2 nA (mean $\pm$ SD, $n = 8$).

The right column of Fig. 5 shows recordings obtained in the same cell after external Ca was replaced by Ba. The traces illustrate that Ba ions flowed through Ca channels better than Ca ions, as indicated by the larger size of the tails. In the range between 0 and $+20$ mV, total Ba conductance was about two times larger than Ca conductance. Ba ions also affected the conductance-voltage relation of Ca channels. Fig. 7 plots the normalized amplitude of tail currents recorded with 10 mM Ca (dots) and 10 mM Ba (squares). A comparison of both curves indicates that external Ba shifted the activation curve 15–20 mV in the negative direction.

Closing kinetics. It has been shown in previous figures that at the instant of repolarization Ca currents were followed by large tail currents. Examples of tails recorded on repolarization to −80 mV after a pulse to +40 mV are shown in Fig. 8 using 10 mM external Ca (*A*) or Ba (*C*) as charge carriers. The decay of the tail current had a clear biphasic time course with a large fast component and a small slow component. The slow component was fitted by an exponential extrapolated to
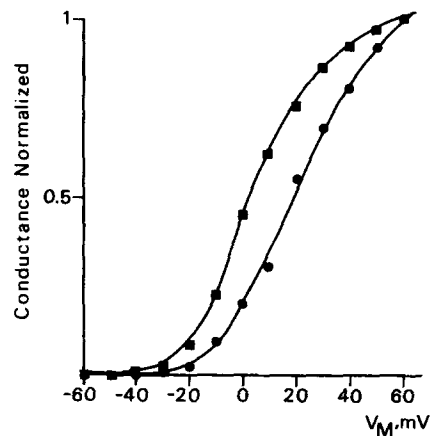

FIGURE 7. Conductance-voltage relation of calcium channels with calcium and barium as charge carriers. Conductance, represented in the ordinate, was measured from the amplitude of tail currents recorded at the instant of repolarization of 10-ms pulses. The pulse membrane potential is represented on the abscissa. Recordings are from the same cell bathed in 10 mM Ca (dots) and 10 mM Ba (squares). Lines were drawn by eye. HP, −80 mV. Solutions (in millimolar): 140 Na, 10 Ca (10 Ba), and TTX//130 Cs. Experiment MZ0288K.

the instant of the repolarization that in the example shown in Fig. 8 A had a time constant of 2.17 ms. Subtraction of this slow component from the total current yielded an isolated fast component with an amplitude about 20 times larger than the slow component, which was fitted by another exponential with a time constant of 0.19 ms. Average time constants for the fast and the slow components measured in several cells in the same experimental conditions were, respectively, 0.16 ± 0.03 and 1.3 ± 0.4 ms (mean ± SD, n = 12). C and D of Fig. 8 show that the time course of the tail current was slowed down in the presence of external Ba. The effect of Ba was more marked on the fast component and therefore the biphasic time course was less pronounced.

These results suggest that, as reported in other preparations (Matteson and Armstrong, 1986) type I cells may have two populations of Ca channels with different deactivation kinetics. The existence of two distinct Ca currents was, however, difficult to reveal by procedures other than tail current measurements (see below).
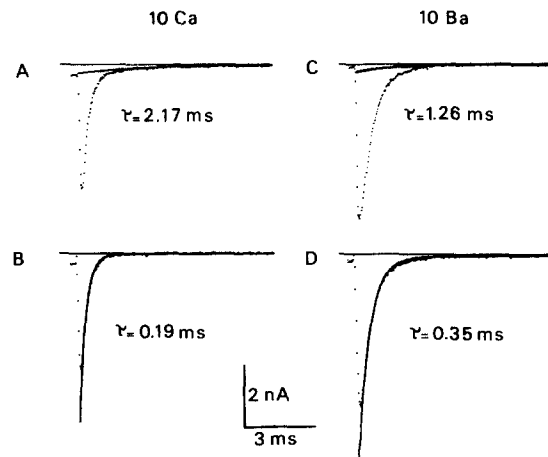

FIGURE 8. Deactivation kinetics of calcium channels with calcium and barium as charge carriers. (A) Tail current recorded after a pulse of 10 ms to 40 mV from a HP of −80 mV. The small and slow component of the tail is fitted by an exponential extrapolated to the instant of the repolarization. Subtraction of the slow exponential from the current yields a fast component (B), which is fitted by a faster and larger exponential. (C and D) Tail currents and exponential fitting with barium ions as charge carriers. Pulse protocol and fitting procedure were conducted as in A and B. The time constants of the different exponentials are indicated next to each trace. Solutions (in millimolar): 140 Na, 10 Ca (10 Ba), and TTX//130 Cs. Experiment MZ0288K.

Inactivation. The time course of the inward Ca current elicited by a 100-ms depolarization is shown in Fig. 9 A. The current reached a maximum in 8–10 ms and thereafter it began to inactivate slowly. At the end of the pulse the amplitude was 73% of the peak value. Fig. 9 B is a family of tail currents recorded in a different cell after pulses to 40 mV. Pulse durations are indicated in milliseconds next to each trace. Tail amplitude decreased with longer pulse durations because of the progressive inactivation of the channels. Numerical values of this experiment are plotted in Fig. 9 C, which illustrates that at the end of 300-ms pulses to 40 mV, Ca conductance is reduced to 27% of the maximal value which is proportional to the amplitude of the tail current.

Is there more than one calcium channel type? It is known that in several mammalian cells there are at least two populations of Ca channels. These channels can be clearly distinguished by their closing kinetic and are classified as fast (FD) and slow
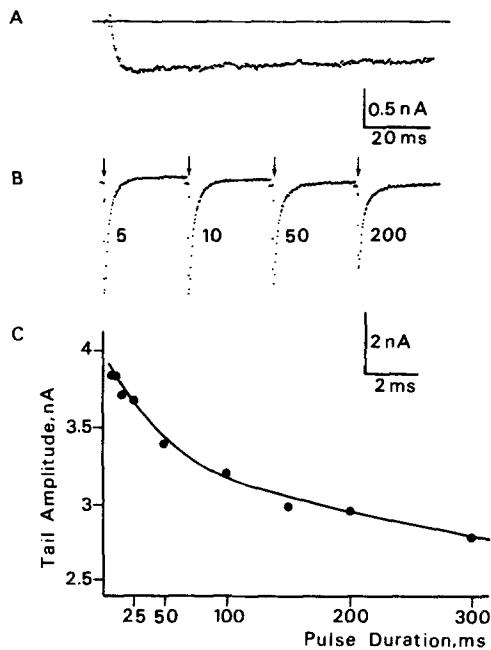
FIGURE 9. Inactivation of the calcium current. (A) Time course of the calcium current during a 100-ms depolarization to 20 mV. HP, −80 mV. (B) Calcium tail currents recorded upon the return to the HP of −80 mV of pulses to 40 mV lasting 5, 10, 50, and 200 ms. The arrows indicate the instant of repolarization. Tail amplitude as a function of pulse duration is plotted in C, which illustrates the progressive inactivation of the current. Experiments MZ0288K (A) and EN2588J (B and C). Solutions (in millimolar): 140 Na, 10 Ca, and TTX//130 Cs.

(SD) deactivating channels (Matteson and Armstrong, 1986). FD channels have a higher threshold and inactivate more slowly than SD channels. In addition, FD channels are rapidly washed out during intracellular dialysis whereas SD channels seem to be resistant to the dilution of cytosolic components.

The decay of Ca tail currents in type I cells had two clear components with single exponential time courses similar to those of SD and FD Ca channels, but evidence favoring the existence of two types of Ca channels were not clearly seen using other experimental protocols. The inactivation time course of the total Ca current showed in Fig. 9 is similar to that of FD channels observed in other cells using equivalent
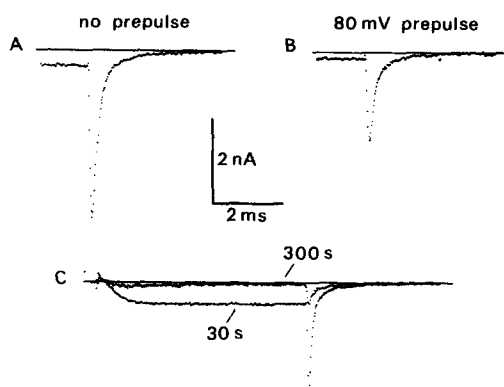
FIGURE 10. (A) Calcium tail current recorded at the end of a 6-ms pulse to 40 mV. The pulse current and the tail decreased in amplitude when the test pulse was preceded by a 500-ms prepulse of 80 mV (B). HP, −80 mV. (C) Wash-out of calcium channels in the absence of exogenous internal Mg-ATP. Both traces were recorded in the same cell during voltage steps to 20 mV delivered 30 and 300 s after the beginning of the whole-cell recording mode. HP, −80 mV. Solutions (in millimolar): 140 Na, 10 Ca, and TTX//130 Cs. Experiments MZ0288K (A and B) and AB1588K (C).

experimental conditions (Cota, 1986; Tabares et al., 1989). Furthermore, Fig. 10 shows that partial inactivation of the Ca current with a 500-ms prepulse to 0 mV (B) produces a decrease in the tail amplitude, but the time course, compared with the trace shown in A, remains almost unchanged. In other preparations, where there exist a large population of SD Ca channels, this same pulse protocol would completely abolish the slow component (Matteson and Armstrong, 1986; Cota, 1986; Tabares et al., 1989). Fig. 10 C illustrates, in a cell dialyzed with a solution without Mg-ATP, the almost total disappearance of the Ca current 300 s after the initiation of the whole-cell recording mode. These results indicate that most of the Ca current in type I cells is due to the activity of FD Ca channels, which, in the absence of internal ATP, rapidly disappear during intracellular dialysis. Although some SD channels may exist they are much less numerous than FD channels and have only a small contribution to the total Ca current generated by the cells.
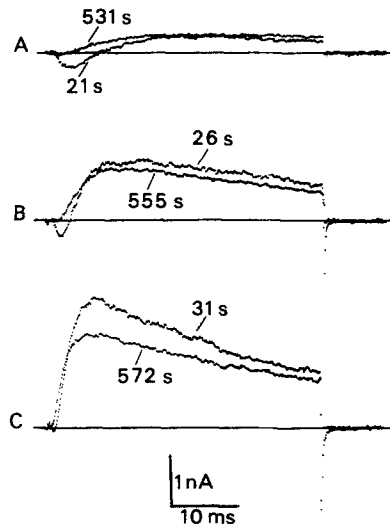
FIGURE 11. Potassium currents recorded before and after wash-out of calcium channels. Current recorded during depolarizations to (A) 0, (B) 20, and (C) 40 mV from a HP of −80 mV. Recordings were obtained in the same cell a few seconds after initiation of the whole-cell recording mode (traces at 21, 26, and 31 s) and ~9 min later (traces at 531, 555, and 572 s). Solutions (in millimolar): 140 Na, 5 Ca, TTX//130 K, no ATP added, and 0.1 μM ionic Ca (3 mM Ca and 5 mM EGTA). Experiment MZ1688J.

Properties of the Potassium Current

Identification of the currents. On depolarization all type I cells dialyzed with a high K solution generated a large voltage-dependent outward K current. Part of this current appears to be Ca-dependent since it decreased in amplitude after the disappearance of functional Ca channels. Most experiments on K currents were therefore performed after wash-out of Ca channels to separate the voltage-dependent component from that activated by Ca influx. In Fig. 11, in a cell treated with TTX, the time course of membrane currents elicited a few seconds after the initiation of the whole-cell recording mode (traces at 21, 26, and 31 s) are compared with currents obtained 8–9 min later (traces at 531, 555, and 572 s). For each pair of traces membrane voltages during the pulse were (A) 0, (B) 20, and (C) 40 mV. This figure illustrates the disappearance of the inward current and the tails after wash-out of Ca channels and the parallel decrease in amplitude of the K current. Once Ca channels were washed out the amplitude of the K current remained stable for more than 20–30 min.

Current-voltage relations and time course. Fig. 12 illustrates the properties of the voltage-dependent K current of type I cells. The current-voltage relation is shown in Fig. 12 A; the peak current amplitude is plotted as a function of the membrane potential. The activation threshold is ~ -20 mV and current amplitude began to saturate at a V_M of 60–70 mV. The K current has a typical sigmoid activation time course (trace B) and at 40 mV reaches a maximum in $\sim$5–10 ms. At this same membrane potential the time to reach half maximal amplitude was 3.4 ± 0.9 ms (mean ± SD, $n = 22$). Traces C and D were obtained with the same pulse amplitude and illustrate that the K current inactivated almost completely during long depolarizations. In the example shown in D the amplitude of the current at the end of the 240-ms pulse was only 12% of the peak value.
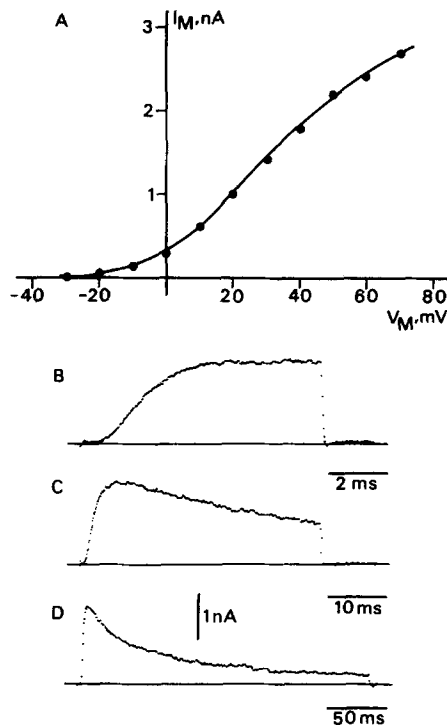

FIGURE 12. Current-voltage relation and time course of the potassium current. (A) Peak current amplitude (ordinate) as a function of the step membrane potential (abscissa). (B–D) Potassium currents recorded during depolarizations to 40 mV lasting (B) 8, (C) 40, and (D) 240 ms. HP, −80 mV. All recordings are from the same cell and were obtained after wash-out of calcium channels. Solutions (in millimolar): 140 Na, 5 Ca, TTX//130 K, no ATP added, and 0.1 µM ionic calcium (3 mM Ca and 5 mM EGTA). Experiment MZ1688J.

Blockade by tetraethylammonium. The K current of type I cells was blocked by the external application of TEA. This is illustrated in Fig. 13 by recordings obtained during (A) 8 and (B) 90-ms pulses to 40 mV. Control and recovery traces show an almost perfect reversibility despite the high concentration of TEA (40 mM) used.

Current-Clamp Recordings

In all type I cells tested ($n > 30$) switching from voltage to current clamp mode caused a fast depolarization and the generation of large action potentials. Some cells fired a single action potential and afterwards reached a steady depolarized membrane potential, but others generated a train of spontaneous spikes. Examples of repetitive firing in two different cells are shown in Fig. 14. The overshoot potential
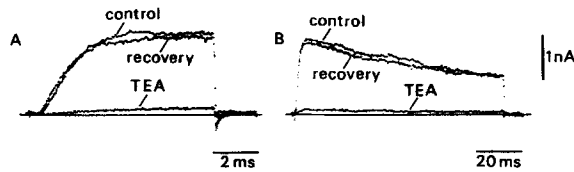
FIGURE 13. Reversible block-ade of the voltage-dependent potassium current by TEA. Currents recorded during (A) 8 and (B) 90-ms step depolari-zations to 40 mV from a hold-ing potential of −80 mV. Solu-tions (in millimolar): 100 Na, 40 TEA, TTX//130 K, no ATP added, and 10 EGTA. Experi-ment MZ1688K.

reached values between 15 and 40 mV and the maximum rate of rise of the action potential upstroke varied from 30 to 100 V/s. An estimate of the peak inward current during an action potential calculated by the formula

$$I = C \cdot dV/dt,$$

yields values from 0.2 to 0.7 nA which are close to the peak inward current ampli-tudes recorded under voltage clamp. The variability in the electrical behavior and in the shape of action potentials of type I cells can be explained by differences in the density of the different ionic currents (see following article), although the magni-tude of the leakage conductance and other uncontrolled variables may also be of importance. These results, expected from the voltage-clamp recordings, directly demonstrate that type I cells are excitable and that under the appropriate condi-tions can repetitively generate large action potentials.
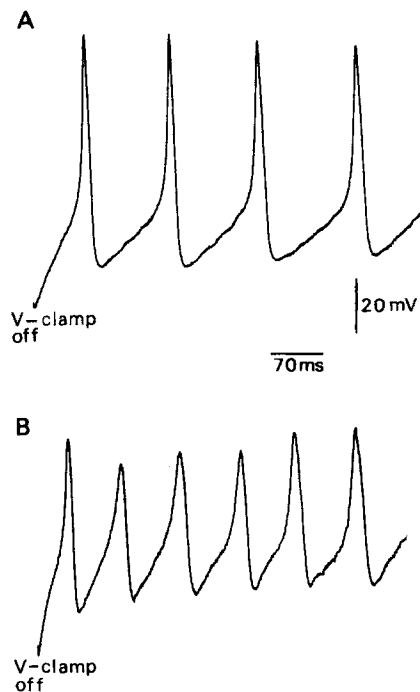

FIGURE 14. Action potentials re-corded spontaneously from type I cells under current-clamp conditions. Traces A and B are from two different cells. Cells were first voltage clamped to a HP of −80 mV for 2–4 min and then the amplifier was switched to current-clamp mode. Solutions (in millimolar): 140 Na, 5 Ca//130 K, 3 Mg-ATP, and 0.1 µM Ca (3 mM Ca and 5 mM EGTA). Experiment MZ2188J.

Electrical Properties of Type II Cells

In some experiments we recorded the ionic currents generated by a second population of cells, considered as putative type II cells, which had a small size and could be clearly differentiated from the larger and more numerous type I cells (see Methods). Recordings from type II cells did not show any indication of the activity of Na and/ or Ca channels that were typical of type I cells. On depolarization type II cells only generated a slowly activating tiny outward current that was probably carried by K ions. The maximal amplitude of the outward current measured at the end of 8-ms pulses to +40 mV varied between 80 and 200 pA ($n = 10$). An example of current recorded in type II cells is shown in Fig. 15. The traces are from a cell with the largest current amplitude so far recorded. The cell was held at −80 mV and current elicited by depolarizations to (A) 0 and (B and C) +40 mV.
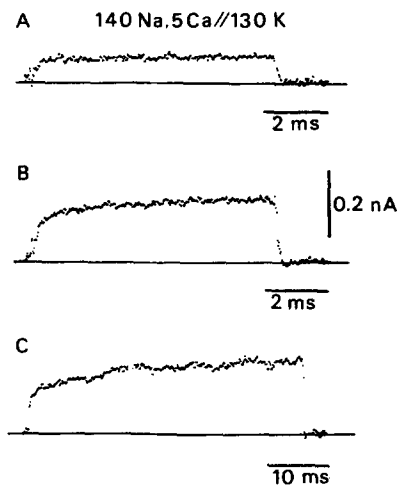
A   140 Na, 5 Ca // 130 K

FIGURE 15. Ionic current in type II cells. (A and B) Currents recorded during voltage steps to (A) 0 and (B) +40 mV with a return to the holding potential of −80 mV after 8 ms. Note the absence of inward current and the generation of a small outward current. (C) Outward current recorded during a depolarization to +40 mV lasting 45 ms. Solution composition was as indicated in the figure. Experiment SE0888J.

DISCUSSION

Our results indicate, from an electrophysiological viewpoint, that in the carotid body there are two clearly distinct types of cells. Type I cells are excitable and have voltage-gated sodium, calcium, and potassium channels, whereas type II cells are unexcitable, electrophysiologically much simpler, and only have a small outward K current. Thus, this section concentrates on the electrophysiology of type I cells.

Type I cells, which are of neuroectodermal origin (Kondo et al., 1982), have been thought to be nonexcitable (Eyzaguirre et al., 1983). We have now found that they can generate large action potentials similar to those found in nerve and other electrically excitable cells. These new findings are of importance for understanding the physiology of type I cells and must be taken into account to explain chemosensory transduction in the carotid body.

Ionic Currents of Type I Cells

Sodium current. Qualitatively the Na current of type I cells is similar to I_{Na} from the squid giant axon (Hodgkin and Huxley, 1952) and from other vertebrate prep-

arations (for example Sah et al., 1988). The current has a fast activation and inacti-
vation, is completely blocked by nanomolar concentrations of TTX, and is selectively
carried by Na ions. Activation of I_{Na} in type I cells is similar to the Na current
recorded in GH$_3$ cells (Matteson and Armstrong, 1984) but is somewhat slower than
the current from the squid axon (Hodgkin and Huxley, 1952; Bezanilla and Arm-
strong, 1977). The peak of the current-voltage curve occurred at 10 mV, which is
similar to Na currents recorded in GH$_3$ (Dubinsky and Oxford, 1984; Matteson and
Armstrong, 1984) and chromaffin (Fenwick et al., 1982) cells, but it is displaced
toward positive voltages if compared with Na currents recorded in neurons (Sah et
al., 1988) and neuroblastoma cells (Moolenaar and Spector, 1978). These quantita-
tive differences were also seen in the voltage-dependence of steady-state inactiva-
tion. In our experiments half of the Na channels were inactivated at ~ −50 mV, a
value similar to that measured in GH$_3$ cells (Dubinsky and Oxford, 1984; Matteson
and Armstrong, 1984), but less negative than the one observed in central neurons
(−75 mV, Sah et al., 1988). Inactivation of Na currents from type I cells follows a
single exponential time course and is relatively fast compared with activation. A sin-
gle exponential decay has also been observed in GH$_3$ cells (Vandenberg and Horn,
1984) although a biexponential time course was required to fit Na inactivation in rat
and frog nerve (Chiu, 1977; Neumcke and Stampfli, 1982). Na current density in
type I cells, assuming that there is no membrane infolding, was 0.15 mA/cm^2. This
value is within the range of the estimations done in GH$_3$ cells (Dubinsky and
Oxford, 1984; Matteson and Armstrong, 1984) but it is about 10 times smaller than
in the squid axon. Thus, on quantitative grounds the Na current of type I cells
resembles the I_{Na} of GH$_3$ and chromaffin cells, but differs in some aspects from the
current existing in neurons and nerve cells.

Despite the existence of a relatively low density of Na channels, type I cells, like
other secretory cells, can generate large action potentials. The fact that in glomus
cells steady-state inactivation of I_{Na} is displaced in the positive direction may contrib-
ute to a more efficient use of the Na channels available (see also Matteson and Arm-
strong, 1984). Resting potentials measured in previous intracellular recordings per-
formed in type I cells were in the neighborhood of −20 mV (Acker and Pietruschka,
1977; Eyzaguirre et al., 1983). Our results show that >90% of g_{Na} is inactivated at
−25 mV, which explains the unexcitability of the intracellularly recorded cells,
which were probably damaged by the microelectrodes.

Calcium current. Blockade of Na channels by TTX revealed in all type I cells the
existence of a Ca current. This current resembles I_{Ca} from other vertebrate prepara-
tions in its time course, its sensitivity to external divalent cation block, and the ability
of Ba to substitute for Ca as charge carrier (Fenwick et al., 1982; Hagiwara and
Ohmori, 1982; Dubinsky and Oxford, 1984; Matteson and Armstrong, 1984). The
peak of the current-voltage curve was at 10–20 mV, which is close to the values
observed in other cells. In equivalent experimental conditions, the amplitude of the
Ca current is somewhat larger in type I cells than in GH$_3$ (Hagiwara and Ohmori,
1982; Dubinsky and Oxford, 1984; Matteson and Armstrong, 1984), chromaffin
(Fenwick et al., 1982), adenohypophysial (Cota, 1986), and pancreatic beta (Hiriart
and Matteson, 1988) cells. With 10 mM external Ca, the peak Ca current amplitude
was almost the same as the maximal Na current.

Indications of the existence of more than one Ca channel type have been observed in a number of secretory cells (Cota, 1986; Matteson and Armstrong, 1986; Hiriart and Matteson, 1988; Tabares et al., 1989), neurons (Carbone and Lux, 1984; Nowycky et al., 1985), and muscle (Bean, 1985). In hypophysial pars intermedia, pancreatic beta cells, and adrenocortical cells, FD and SD Ca channels are distinguished according to their different closing kinetics. FD channels also have a higher threshold and inactivate more slowly than SD channels. Ca tails in most type I cells follow a clear biphasic time course and are well fitted by the sum of a small slow exponential and a fast larger exponential. The time constants of the two components are comparable to those measured in other preparations (Cota, 1986; Matteson and Armstrong, 1986).

Although the analysis of the deactivation kinetics of Ca currents suggests the existence in type I cells of two Ca channel types, a number of experimental observations do not support this interpretation. (*a*) Ca current of type I cells inactivate very slowly with a time course that resembles that of FD channels from other preparations. (*b*) The time course of tail currents recorded after short and large depolarizations is similar and is not affected by a 500-ms conditioning prepulse. In other cells the slow component of the tails, which represents the closing of SD channels, is markedly reduced after long (>50 ms) depolarizations or by a conditioning depolarizing prepulse. (*c*) The conductance-voltage relation with Ba ions as charge carriers is displaced 15–20 mV toward negative voltages. Ba also slows down the closing of the channels. These effects of Ba are known to be mediated by their interaction with FD channels. Finally, (*d*) in the absence of exogenous internal Mg-ATP the Ca current of glomus cells is very labile and disappears almost completely in 5–8 min. This property is typical of FD channels whereas SD channels seem to be resistant to dilution of cytosolic components (Cota, 1986; Matteson and Armstrong, 1986).

All together this evidence indicates that Ca current in type I cells is mainly mediated by FD channels. A small population of SD channels, responsible for the slow component of the tails, may exist but unequivocal proofs for their existence were not found. The possibility still remains that the slow component of the tails is either a result of the activity of Ca channels that are different from SD channels, or that it represents a particular kinetic property of FD channels in type I cells.

Potassium current. An outward K current was recorded in all type I cells studied. This current was recorded with a large amplitude in cells with internal Ca concentrations ranging between 0.5 μM and $<10^{-10}$ M, but in a given cell it decreased in amplitude after wash-out of Ca channels. Thus, a percentage of this current may be due to the activity of Ca-dependent K channels activated by the local rise in cytosolic Ca that follows Ca influx through functional Ca channels (Marty and Neher, 1985). Because of the rapid disappearance of Ca channels in our preparation, even in the presence of 3 mM internal Mg-ATP, we centered on the study of the voltage-dependent K current after wash-out of Ca channels.

The voltage-dependent K current of type I cells has a typical sigmoid activation time course, at +40 mV it reaches half maximal amplitude in 3.5 ms, and thereafter it slowly inactivates. The current is qualitatively similar to delayed K currents from other preparations (Adrian et al., 1970; Dubinsky and Oxford, 1984; Rorsman and Trube, 1986; Matteson and Carmeliet, 1988). It is, however, slower than K currents

of the squid axon or neurons dispersed from the squid giant fiber lobe (Hodgkin and Huxley, 1952; Armstrong and López-Barneo, 1987), but its activation time course is similar to current from vertebrate secretory cells (Dubinsky and Oxford, 1984; Rorsman and Trube, 1986). The K current in type I cells inactivated almost completely in 250 ms. This same behavior is found in K currents from a number of preparations including squid neurons (Llano and Bookman, 1986), GH₃ cells (Matteson and Carmeliet, 1988), and skeletal muscle fibers (Adrian et al., 1970). The voltage-dependent K current of type I cells was, as were other K currents, almost abolished by a large concentration of external TEA. In our experiments the reversibility of the TEA blockade was almost perfect.

Possible Participation of Ionic Channels in the Physiology of Type I Cells

Although type I cells have been considered the best candidates for being the primary chemoreceptors since the early work on the carotid body, the basic mechanisms involved in this process have remained largely unknown (for a review see Belmonte and González, 1983). Recent investigations have shown that both hypoxia and high external potassium, which presumably causes membrane depolarization, produce secretion of dopamine in the carotid body and that this effect is abolished by Ca channel antagonists (Fidone et al., 1982; Almaraz et al., 1986; Obeso et al., 1987). Thus, type I cells may function in a way similar to other secretory systems in which Ca influx through voltage-gated membrane Ca channels is a critical event leading to secretion. This idea could not be reconciled with the fact that type I cells impaled with microelectrodes were found to be unexcitable (Eyzaguirre et al., 1983), however, the results shown in this article demonstrate that they have an appreciable density of voltage-dependent sodium and calcium channels and that they can repetitively generate action potentials. Na channels have, therefore, an important role in spike generation and by producing a fast depolarization contributes to the opening of Ca channels, which are well suited for fast injection of Ca into the cytosol. The Ca-activated component of the K current may participate in spike repolarization, whereas the slowly inactivating K channels are most probably involved in pacemaking.

The findings reported here led us to hypothesize that ionic channels in type I cells might be regulated by environmental O₂ tension and that they might therefore be directly implicated in chemotransduction. This hypothesis was experimentally confirmed as illustrated in the following article.

REFERENCES

Acker, H., and F. Pietruschka. 1977. Meaning of the type I cell for the chemoreceptive process. An electrophysiological study on cultured type I cells of the carotid body. *In* Chemoreception in the

Carotid Body. H. Acker, S. Fidone, D. Pallot, C. Eyzaguirre, D. W. Lübbers, and R. W. Torrance, editors. Springer-Verlag, Berlin. 92–98.

Adrian, R. H., W. K. Chandler, and A. L. Hodgkin. 1970. Slow changes in potassium permeability in skeletal muscle. *Journal of Physiology.* 208:645–688.

Almaraz, L., C. González, and A. Obeso. 1986. Effects of high potassium on the release of ^{3}H-dopamine from the cat carotid body in vitro. *Journal of Physiology.* 379:293–307.

Armstrong, C. M., and J. López-Barneo. 1987. External calcium ions are required for potassium channel gating in squid neurons. *Science.* 236:712–714.

Bean, B. P. 1985. Two kinds of calcium channels in canine atrial cells. Differences in kinetics, selectivity, and pharmacology. *Journal of General Physiology.* 86:1–30.

Belmonte, C., and C. González. 1983. Mechanisms of chemoreception in the carotid body: possible models. *In* Physiology of the Peripheral Arterial Chemoreceptors. H. Acker and R. G. O'Reagan, editors. Elsevier Science Publishing Co., Inc., Amsterdam. 197–220.

Bezanilla, F., and C. M. Armstrong. 1977. Inactivation of the sodium channel. I. Sodium current experiments. *Journal of General Physiology.* 70:549–566.

Carbone, E., and H. D. Lux. 1984. A low voltage–activated, fully inactivating Ca channel in vertebrate sensory neurons. *Nature.* 310:501–502.

Chiu, S. Y. 1977. Inactivation of sodium channels: second order kinetics in myelinated nerve. *Journal of Physiology.* 273:573–596.

Cota, G. 1986. Calcium channel currents in pars intermedia cells of the rat pituitary gland. *Journal of General Physiology.* 88:83–105.

De Castro, F. 1928. Sur la structure et l'innervation du sinus carotidien de l'homme et des mammiféres. Nouveaux faits sur l'innervation et la fonction du glomus caroticum. Etudes anatomiques et physiologiques. *Trabajos del Laboratorio de Investigaciones Biológicas de la Universidad de Madrid.* 25:331–380.

Dubinsky, J. M., and G. S. Oxford. 1984. Ionic currents in two strains of rat anterior pituitary tumor cells. *Journal of General Physiology.* 83:309–339.

Eyzaguirre, C., L. Monti-Bloch, Y. Hayashida, and M. Barón. 1983. Biophysics of the carotid body receptor complex. *In* Physiology of the Peripheral Arterial Chemoreceptors. H. Acker and R. G. O'Reagan editors. Elsevier Science Publishing Corp., Inc., Amsterdam. 59–88.

Eyzaguirre, C., and P. Zapata. 1968. A discussion of possible transmitter or generator substances in carotid body chemoreceptors. *In* Arterial Chemoreceptors. R. W. Torrance editor. Blackwell Scientific Publications, Inc., Oxford. 213–251.

Fenwick, E. M., A. Marty, and E. Neher. 1982. Sodium and calcium channels in bovine chromaffin cells. *Journal of Physiology.* 331:599–635.

Fidone, S. and C. González. 1986. Initiation and control of chemoreceptor activity in the carotid body. *In* Handbook of Physiology. The Respiratory System II. A. P. Fishman, editor. American Physiological Society, Bethesda, MD. 247–312.

Fidone, S., C. González, and K. Yoshizaki. 1982. Effects of low oxygen on the release of dopamine from the rabbit carotid body in vitro. *Journal of Physiology.* 333:93–110.

Fitzgerald, R. S., and S. Lahiri. 1986. Reflex responses to chemoreceptor stimulation. *In* Handbook of Physiology. The Respiratory System II. A. P. Fishman, editor. American Physiological Society, Bethesda, MD. 313–362.

Forscher, P., and G. S. Oxford. 1985. Modulation of calcium channels by norepinephrine in internally dialyzed avian sensory neurons. *Journal of General Physiology.* 85:743–763.

Hagiwara, S., and H. Ohmori. 1982. Studies of calcium channels in rat clonal pituitary cells. *Journal of Physiology.* 336:649–661.

Hamill, O. P., A. Marty, E. Neher, B. Sakmann, and F. S. Sigworth. 1981. Improved patch-clamp

techniques for high-resolution current recording from cells and cell-free membrane patches. *Pflügers Archiv.* 391:85–100.

Heymans, C., J. J. Bouckaert, and L. Dautrebande. 1930. Sinus carotidien et réflexes respiratoires. II. Influences respiratoires réflexes de l'acidôse, de l'alcalôse, de l'anhydride carbonique, de l'ion hydrogène et de l'anoxémie: sinus carotidiens et échanges respiratoires dans les poumons et au delà des poumons. *Archives Internationales de Pharmacodynamie et de Thérapie.* 39:400–408.

Hiriart, M., and D. R. Matteson. 1988. Na channels and two types of Ca channels in rat pancreatic B cells identified with the reverse hemolytic plaque assay. *Journal of General Physiology.* 91:617–639.

Hodgkin, A. L., and A. F. Huxley. 1952. A quantitative description of membrane current and its application to conduction and excitation in nerve. *Journal of Physiology.* 117:500–544.

Kondo, H., T. Iwanaga, and T. Nakajima. 1982. Immunocytochemical study on the localization of neuron specific enolase and S-100 proteins in the carotid body of rats. *Cell and Tissue Research.* 227:291–295.

Kostyuk, P. G. 1984. Metabolic control of ionic channels in the neuronal membrane. *Neuroscience.* 13:983–989.

Liu, Y., and G. A. Gibson. 1986. Microcomputer Systems: the 8086/8088 Family. Architecture, Programming and Design. Prentice Hall, Inc., NJ.

Llano, I., and R. S. Bookman. 1986. Ionic conductances of squid giant fiber lobe neurons. *Journal of General Physiology.* 88:543–569.

López-Barneo, J., J. R. López-López, J. Ureña, and C. González. 1988. Chemotransduction in the carotid body: K current modulated by pO_2 in type I chemoreceptor cells. *Science.* 241:580–582.

Matteson, D. R., and C. M. Armstrong. 1984. Na and Ca channels in a transformed line of anterior pituitary cells. *Journal of General Physiology.* 83:371–394.

Matteson, D. R., and C. M. Armstrong. 1986. Properties of two types of calcium channels in clonal pituitary cells. *Journal of General Physiology.* 87:161–182.

Matteson, D. R., and P. Carmeliet. 1988. Modification of K channel inactivation by papain and N-bromoacetamide. *Biophysical Journal.* 53:641–645.

Marty, A., and E. Neher. 1985. Potassium channels in cultured bovine adrenal chromaffin cells. *Journal of Physiology.* 367:117–141.

Moolenaar, W. H., and I. Spector. 1978. Ionic currents in cultured mouse neuroblastoma cells under voltage-clamp conditions. *Journal of Physiology.* 278:265–286.

Neumcke, B., and R. Stampfli. 1982. Sodium currents and sodium current fluctuations in rat myelinated nerve fibres. *Journal of Physiology.* 329:163–184.

Nowycky, M. C., A. P. Fox, and R. W. Tsien. 1985. Three types of neuronal calcium channel with different calcium agonist sensitivity. *Nature.* 316:440–443.

Obeso, A., S. Fidone, and C. González. 1987. Pathways for calcium entry in type I cells of the carotid body. Significance for the secretory response. *In* Chemoreceptors in Respiratory Control. J. A. Ribeiro and D. Pallot, editors. Croom Helm, London. 91–98.

Peatman, J. B. 1977. Microcomputer-Based Design. McGraw-Hill Book Co., New York.

Rorsman, P., and G. Trube. 1986. Calcium and delayed potassium currents in mouse pancreatic β-cells under voltage-clamp conditions. *Journal of Physiology.* 374:531–550.

Sah, P., A. J. Gibb, and P. W. Gage. 1988. The sodium current underlying action potentials in guinea pig hippocampal CA1 neurons. *Journal of General Physiology.* 91:373–398.

Sigworth, F. J. 1983. Electronic design of the patch-clamp. *In* Single Channel Recording. B. Sakmann and E. Neher, editors. Plenum Publishing Corp., New York. 3–35.

Tabares, L., J. Ureña, and J. López-Barneo. 1989. Properties of calcium and potassium currents of clonal adrenocortical cells. *Journal of General Physiology.* 93:495–519.

Ureña, J., J. C. Mateos, and J. López-Barneo. 1989. Low-cost system for automated acquisition, display, and analysis of transmembrane ionic currents. Medical and Biological Engineering and Computing. 27:94–100.

Vandenberg, C. A., and R. Horn. 1984. Inactivation viewed through single sodium channels. *Journal of General Physiology.* 84:535–564.